BULLETIN OF THE EARTHQUAKE
RESEARCH INSTITUTE
Vol. 44 (1966), pp. 1449-1464

70. *Vertical Displacement in a Tsunami Source Area and the Topography of the Sea Bottom.*

By Tokutaro HATORI,

Earthquake Research Institute.

(Read April 26, 1966.—Received Sept. 30, 1966.)

Abstract

Tsunami sources for the Kanto Earthquake of 1923, and the Boso-oki Earthquake of 1953 are estimated by means of an inverse refraction diagram. The former includes the whole of the elevated region at Miura and Boso Peninsula, the latter being located in the region which corresponds to the area of aftershock activity.

The estimated source areas of tsunamis which were generated in the adjacent sea to Japan, are drawn on a bathymetric chart. The mean slope of the sea bottom in the vicinity of each source was of the order of 1/100~1/10. Tsunami energy seems to be affected by the slope of the sea bottom as well as the water depth at the source.

The amount of the sea bottom deformation was estimated from the distribution of the inundation height of a tsunami along the coast. The average vertical displacement in the tsunami source is calculated by using the tsunami energy and the source area. The values thus obtained were of the order of several meters for large earthquakes.

1. Introduction

For the Sanriku Tsunami of 1933, the source area was estimated by N. Miyabe[1] by means of an inverse refraction diagram. He found that the estimated source was very large and could not be approximated by a point source. Since then, many workers[2)-12)] have tried by the same method to estimate the source areas of tsunamis which occurred in adjacent seas to Japan.

According to K. Iida[7], there is a close relationship between the source area of a tsunami, the area of aftershock activity, and the earthquake magnitude. He also indicated that there is some relation between the tsunami magnitude and the water depth at the earthquake epicenter.[13] The effect of the bottom slope on the tsunami generation

was discussed theoretically by K. Nakamura and M. Suzuki.[14] As for the amount of vertical displacement of the sea bottom at the time of earthquake, K. Iida[15] and H. Watanabe[16] attempted to estimate the initial wave height of a tsunami at the source for several tsunamis and obtained the displacement of the order of several meters.

In the present paper, the author has attempted the followings: 1) All the estimated source areas of tsunamis including those newly estimated by the author are compiled on a bathymetric chart to see the geographic distribution of the source areas in relation to the bottom topography. 2) The effect of the bottom slope on tsunami generation is examined, taking the ratio of seismic wave energy to tsunami energy as a parameter. 3) The correspondence is discussed between the vertical crustal displacement surveyed on land along the coast, and the initial wave height of the tsunami estimated at the margin of the tsunami source, where the initial wave height is calculated by applying the ordinary refraction and shoaling coefficients to the inundation height. 4) The average vertical displacement of the sea bottom in the source area is estimated on the basis of the energy consideration, and compared with the amount of the observed crustal deformation on land.[17]

2. Source areas of the tsunamis accompanying the Kanto and Boso-oki Earthquakes

For the Kanto Earthquake of 1923[18] and the Boso-oki Earthquake of 1953,[19] the source areas of tsunamis are estimated by means of an inverse refraction diagram. For the Kanto Earthquake, inverse refraction diagrams are drawn as shown in Fig. 1 from eight tide-gauge stations at Ayukawa, Onahama, Nakaminato, Choshi, Chiba, Tokyo, Owase and Kushimoto, and from Shimoda where the initial arrival was observed by eye-witnesses. Wave fronts were drawn at every two minute intervals, but in Fig. 1 only the final wave front corresponding to the travel time is shown. A reliable estimate of the area is rather difficult because the available tide-gauge stations are located at long distances from the source. However, the estimated area seems reasonable because the whole of the elevated region in Miura and Boso Peninsula are included. The linear dimension of the tsunami domain is about 170 km. Fig. 1 also shows the distribution of the maximum inundation heights in meters.

For the Boso-oki Tsunami of 1953, the source area is obtained as shown in Fig. 2. The mareograms used are of the following ten stations:

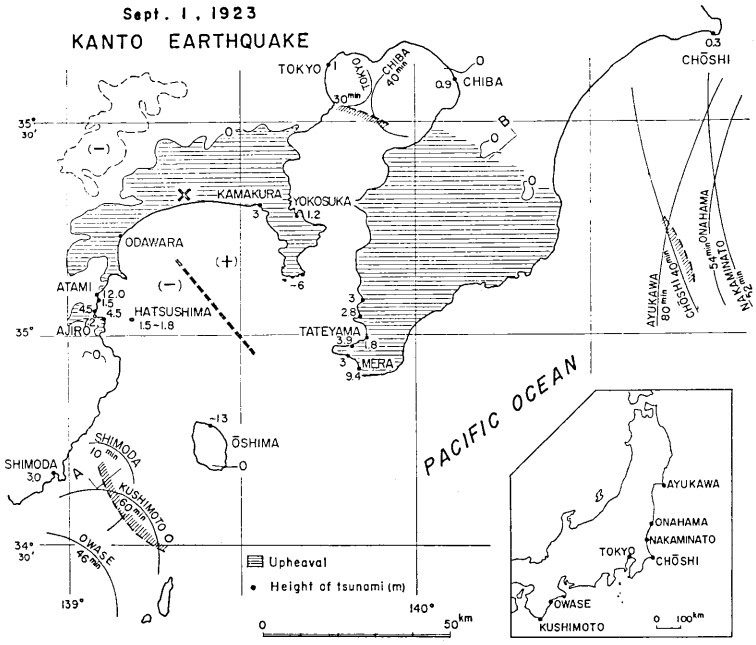

Fig. 1. The source area and the distribution of the inundation height in m, for the tsunami due to the Kanto Earthquake.

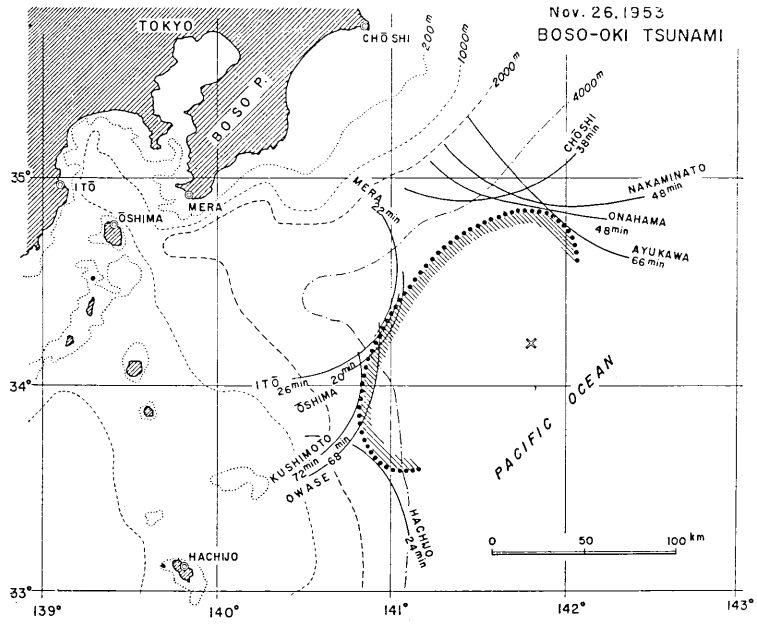

Fig. 2. The source area of the Boso-oki Tsunami.

Ayukawa, Onahama, Nakaminato, Choshi, Mera, Izu-oshima, Ito, Hachijo Island, Owase and Kushimoto. The initial wave front corresponding to the travel time at each station is shown in Fig. 2. The source area of the tsunami is located in the region which corresponds to the area of aftershock activity, extending about 160 km in an elongated shape.

3. Topography of the sea bottom in the source area

For twenty-two tsunamis generated in the adjacent sea to Japan, the estimated source areas are shown on a bathymetric chart (Fig. 3) in which the numeral at the epicenter of each earthquake is the serial number in Table 1. Generally speaking, the source areas lie on a continental slope but some are located in the ocean trench (the Sanriku, Kamchatka and Iturup Earthquakes) and some are located partly on land (the Kanto and Oga Earthquakes). It seems that in Fig. 3 large tsunamis are generated under the deep sea.

Fig. 4 shows examples of the sea bottom topography near the tsunami source. The major axis of source is divided into ten equal widths, where an arrow indicates the location of the main shock. The mean slope of the sea bottom for all tsunamis indicated in Table 1, is of the order of 1/100~1/10.

To discuss the effect of the slope on tsunami generation, the ratio of seismic wave energy E_s to tsunami energy E_t is taken as a parameter. For most of the tsunamis considered, E_s/E_t were calculated by K. Iida,[15] but the author added new data of E_t and E_s/E_t as shown in Gothic type in Table 1. These values are calculated by a formula given by R. Takahasi[20] as follows: Making use of mareograms, the tsunami energy is calculated by

$$E_t=\pi\rho g VR\sum_{n=1}^{\infty}a_n^2T_n, \tag{1}$$

where ρ is the density of sea water, R the distance from the source, V the velocity of tsunami waves at the source, a_n the amplitude, T_n the half-period of tsunami waves and N the total number of wave crests considered. The seismic energy is given by Gutenberg and Richter (1956) as follows:

$$\log E_s=11.8+1.5M, \tag{2}$$

where M is the earthquake magnitude.

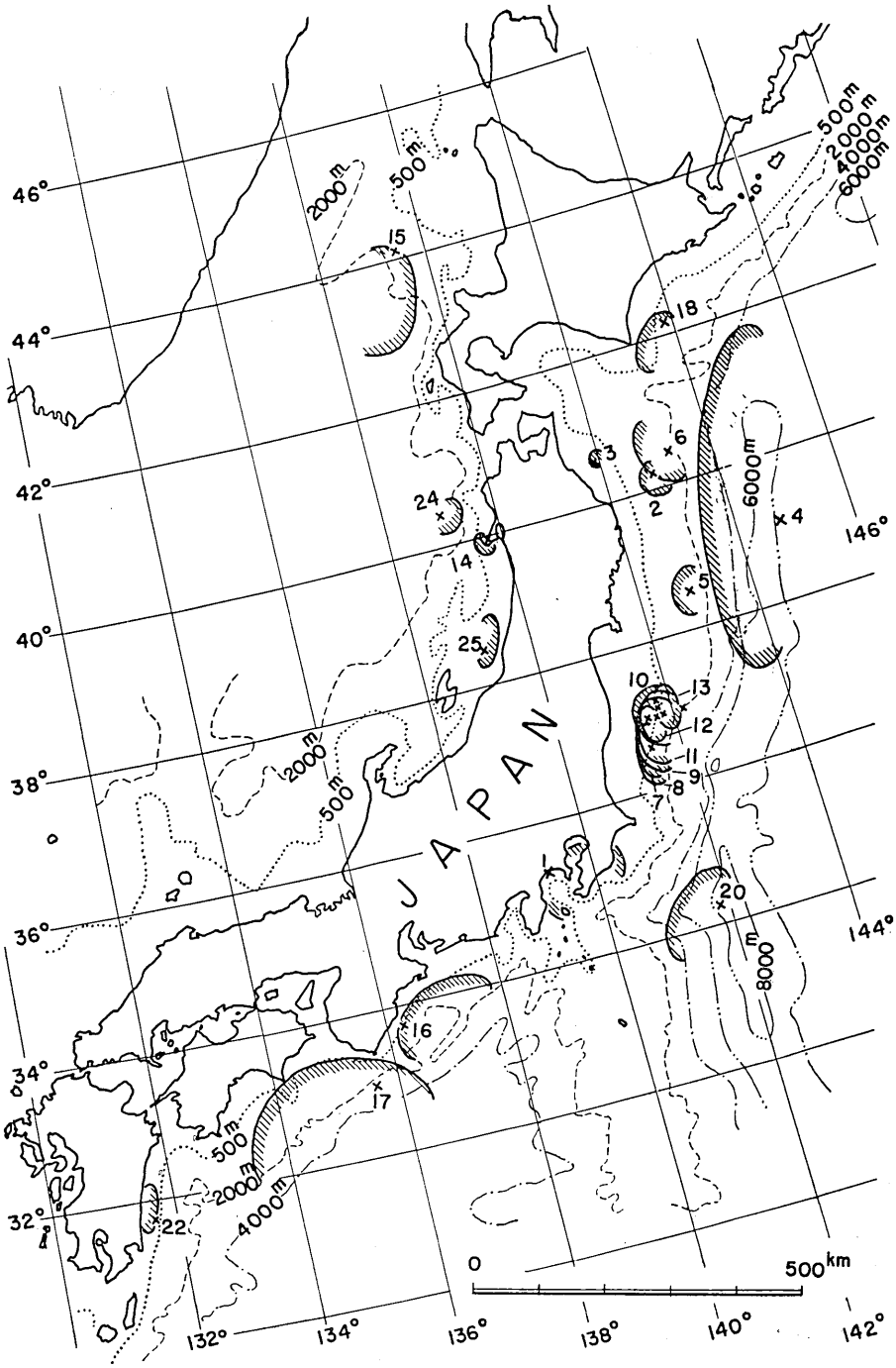

Fig. 3. Distribution of the estimated source area of tsunami generated in the adjacent sea to Japan during the last 40 years.

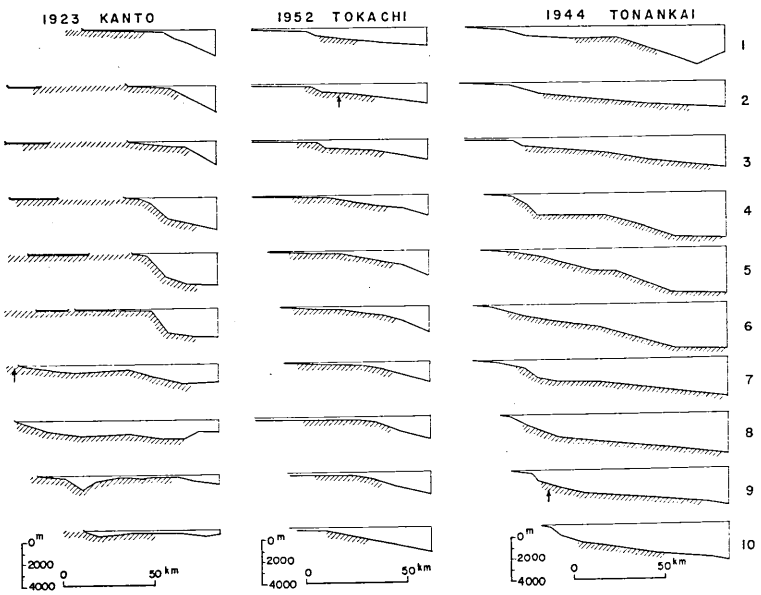

Fig. 4. Examples of the sea bottom topography near the tsunami source.

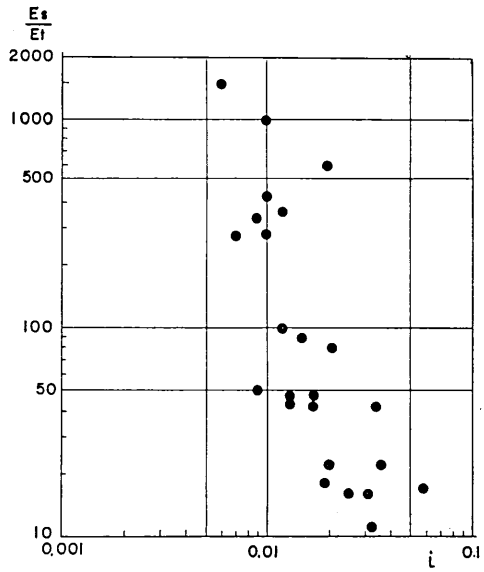

Fig. 5. Relation between the slope of the sea bottom and the ratio of the seismic wave energy, E_s, to the tsunami energy, E_t.

Fig. 5. shows the relation between the mean slope of the sea bottom i and E_s/E_t. Though the plotted points are widely scattered, the tendency is that the larger the slope of the sea bottom, the smaller becomes the ratio of seismic wave energy to tsunami energy. It may be added here that K. Iida[15] suggested that the greater the earthquake magnitude, the smaller becomes E_s/E_t.

4. Sea level disturbances at the margin of tsunami source

On the tsunami due to the Niigata Earthquake,[21] the distribution of the inundation heights along the coast near the generating area corresponded approximately to that of the observed bottom deformation. Taking this fact into consideration, for the cases of following tsunamis, the distribution of the actual deformation of land along the coast is compared with the estimated sea level disturbances at the margin of the tsunami source, where wave-heights at the margin of the source are calculated from the inundation height by applying the refraction and shoaling coefficients. Since we have little data on the initial wave-height at the coast, the inundation heights were used in the calculation.

The Tonankai Tsunami of 1944

Fig. 6 shows a refraction diagram, the distribution of inundation

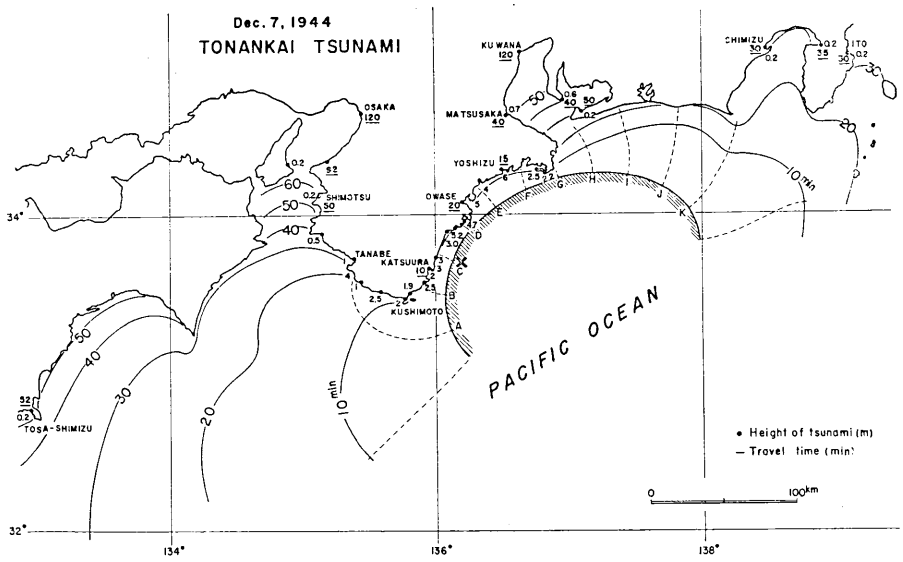

Fig. 6. Refraction diagram, distribution of the inundation height in m, and travel time in min, for the Tonankai Tsunami.

heights and travel time of wave fronts. The source area of this tsunami was obtained by S. Omote.[4] The method of estimating wave height at the margin of the source is as follows: Wave fronts are drawn starting from the margin of the source, at every two minute intervals, but in Fig. 6 only those for every ten minute intervals are shown. For the calculation of the refraction coefficient, the margin of the source was divided into ten equal widths, the coast being taken to be 10 meters deep. For the shoaling coefficient, Green's formula is applied.

Fig. 7 shows the distribution of the calculated wave-heights, η, at the margin of the source and corresponding land displacement, Z, along the coast. The inundation height and travel time are shown in the lower figure of Fig. 7. From Fig. 7, the sea bottom deformation seems to be simple upheaval.

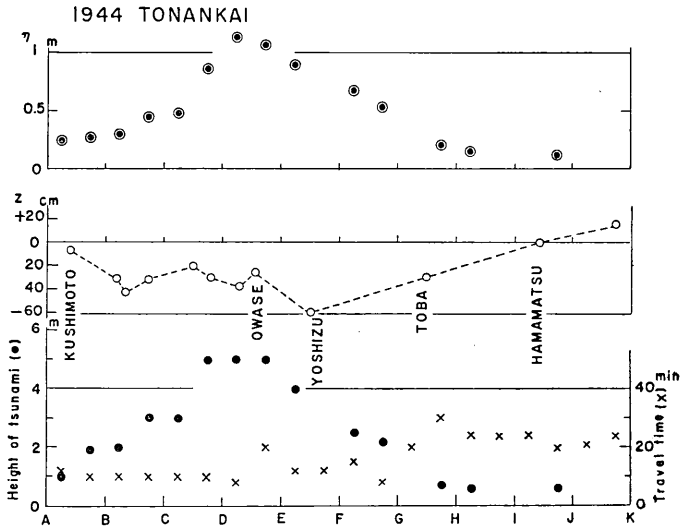

Fig. 7. Calculated wave-heights, η, at the margin of a source and the corresponding crustal deformation, Z, along the coast, for the Tonankai Tsunami.

The Nankaido Tsunami of 1946

Fig. 8 shows a refraction diagram, the distribution of inundation heights and travel time of wave fronts. The source area of this tsunami was obtained by S. Omote.[5] Wave-heights at the margin of the source are calculated in like manner. The distribution of inundation heights

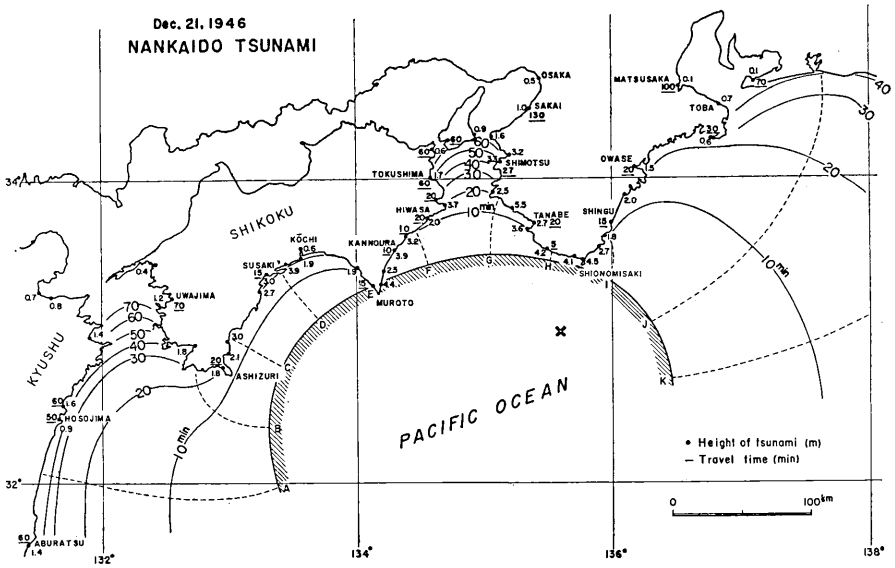

Fig. 8. Refraction diagram, distribution of the inundation height in m, and travel time in min, for the Nankaido Tsunami.

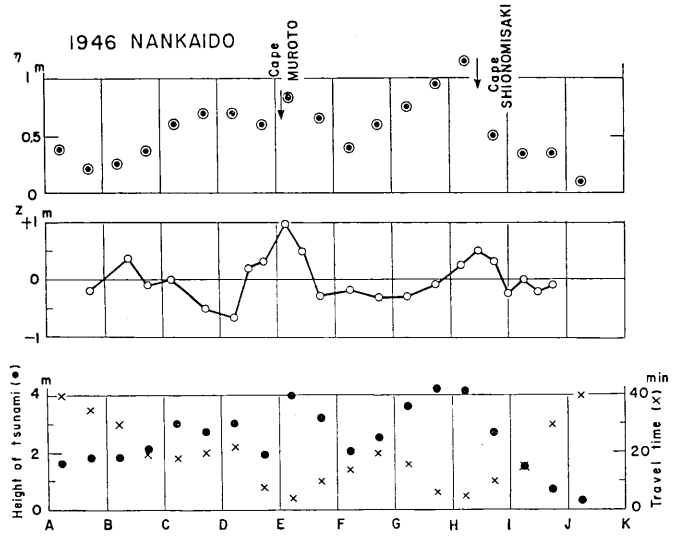

Fig. 9. Calculated wave-heights, η, at the margin of a source and the corresponding crustal deformation, Z, along the coast, for the Nankaido Tsunami.

and land displacement along the coast would depend on the distance from the tsunami source. Two capes lie in or near the source, however, and the calculated wave-heights are related to the observed displacements on land as shown in Fig. 9. From this result, the sea bottom deformation within the tsunami source seems to consist of two regions of upheaval.

The Tokachi-oki Tsunami of 1952

Fig. 10 shows the refraction diagram. The source area has been determined accurately by Z. Suzuki and K. Nakamura[6], because the final wave front agrees approximately with the travel time as shown in Fig. 10. As seen in Fig. 11, the calculated wave-heights are roughly of a similar pattern as the land level change which was deduced from the surveys in 1908 and 1952 by the Japan Geographical Survey Institute.

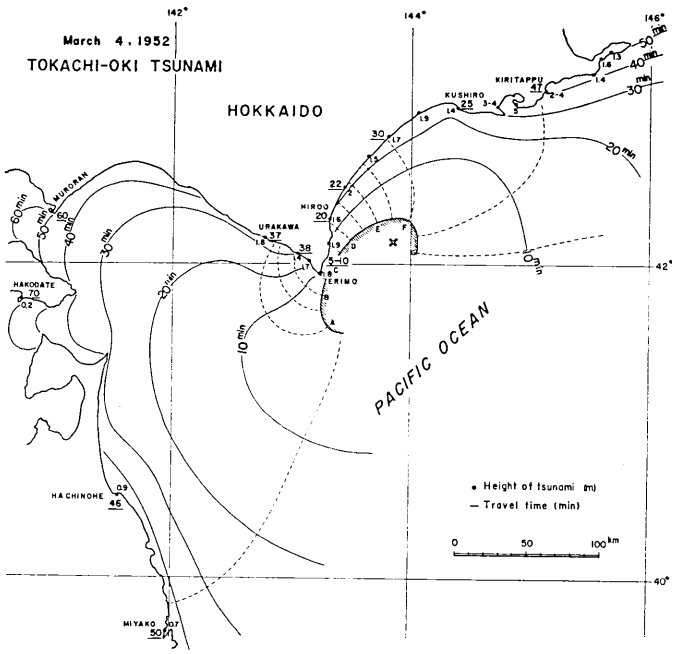

Fig. 10. Refraction diagram, distribution of the inundation height in m, and travel time in min, for the Tokachi-oki Tsunami.

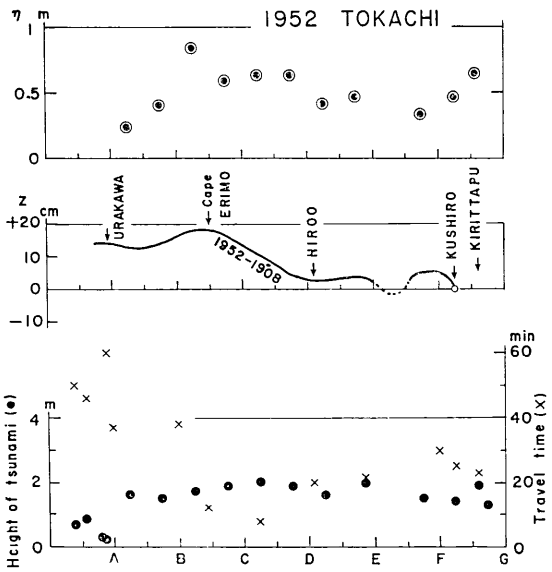

Fig. 11. Calculated wave-heights, η, at the margin of a source and the corresponding crustal deformation, Z, along the coast, for the Tokachi-oki Tsunami.

The Kanto Earthquake of 1923

At the coast in Sagami Bay, the inundation heights on both the

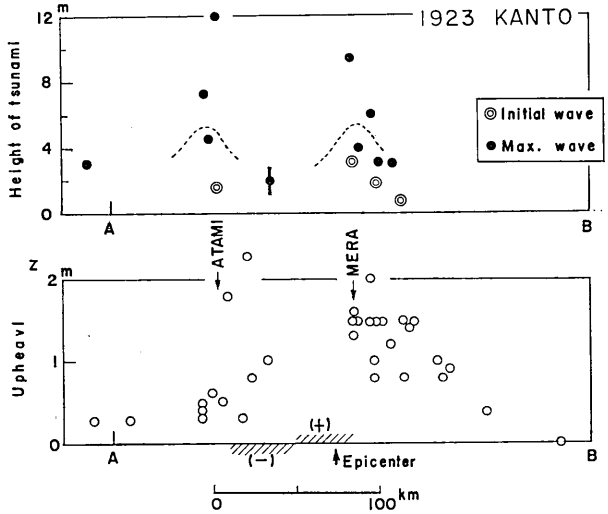

Fig. 12. Profiles of inundation heights and the crustal deformation along a line from A to B in Fig. 1, for the Kanto Earthquake.

eastern and western regions are higher than the central part (Odawara-Kamakura) as shown in Fig. 1. A broken line in Sagami Bay in Fig. 1 shows the boundary of upheaval and subsidence of the sea bottom, which was deduced from the data surveyed by the Japan Hydrographic Office. According to a geological investigation, faults in the sea bottom seem to lie, approximately, in parallel to this boundary. The distribution of inundation heights projected on the profile from A to B in Fig. 1, has two peaks which correspond to the regions of upheaval and subsidence as shown in Fig. 12. Thus, the distribution of inundation heights in the source seems to be related to the sea bottom deformation.

5. Estimation of the vertical displacement in a tsunami source

Making use of tsunami energy, E_t, which is calculated from tsunami waves observed by tide-gauges, and the estimated source area of tsunami, S, the average vertical displacement in the source can be estimated as follows: The potential energy of the sea level disturbance at the source is given by

$$\frac{1}{2}\rho g\int_S \eta^2 dS, \tag{3}$$

where η is the vertical displacement of the water surface at the small portion dS of the dislocated area. Now, if the sea bottom deformation, Z, is completed in a short time interval, we may assume $Z=\eta$ and writing

$$\int_S \eta^2 dS = \bar{Z}^2 S,$$

we have

$$E_t = \frac{1}{2}\rho \bar{Z}^2 S. \tag{4}$$

Results of calculation of the average vertical displacement of the sea bottom, $\sqrt{\bar{Z}^2}$, in the source are shown in Table 1.

Fig. 13 shows the relation between the average vertical displacement in the source and the earthquake magnitude. Although the plotted points are widely scattered, roughly speaking, the average displacement in the source can be estimated from the figure. The hollow circles in Fig. 13 show the values computed by K. Iida,[15] who used the data of aftershock areas instead of the generating areas of tsunamis in (4).

Table 1. List of tsunamis. i: The mean slope of the sea bottom, S: Area of a tsunami source, Z: Calculated vertical displacement in the tsunami source.

No.	Earthquake			Tsunami energy E_t	$\frac{E_s}{E_t}$	i	S	Z	Observed max. displacement	Initial wave
	Date	Location	M	$\times 10^{22}$ergs			$\times 10^3$km^2	(m)	(m)	Up or Down
1	1923 Sept. 1	Kanto	7.9	0.16	279	0.007	12	1.6	−1.0～+1.4	+
2	1928 May 27	Iwate	7.0	**0.007**	286	0.01	2.3	0.8		−
3	1931 Mar. 9	E. Aomori	7.0	**0.002**	1000	0.01	0.4	1.0		+
4	1933 Mar. 3	Sanriku	8.3	15～18	11	0.032	57	7.3～8.2		+
5	1933 June 19	Miyagi	7.1	**0.007**	360	0.012	3.8	0.6		+
6	1935 Oct. 13	Iwate	7.2	0.04	100	0.012	7.4	0.3		+
7	1938 May 23	Ibaraki	7.1	0.06	47	0.017	4.8	0.5		+
8	1938 Nov. 5	Ibaraki	7.7	0.25	80	0.021	8.8	2.4		+
9	1938 Nov. 5	Ibaraki	7.6	**0.074**	90	0.015	7.4	1.4		+
10	1938 Nov. 6	Fukushima	7 5	**0.027**	47	0.013	7.0	0.9		−
11	1938 Nov. 7	Fukushima	7.1	0.06	42	0.017	8.5	0.4		+
12	1938 Nov. 14	Fukushima	7.0	0.047	43	0.014	1.6	2.4		+
13	1938 Nov. 22	Fukushima	6.7	0.04	18	0.019	3.1	1.6		−
14	1939 May 1	Oga	6.7	**0.0004**	1500	0.006	0.6	0.4	+0.4	+
15	1940 Aug. 2	W. Hokkaido	7.5	**0.03**	330	0.023	16	0.6		+
16	1944 Dec. 7	Tonankai	8.0	7.9～8.8	16	0.031	14	10.7～11.3	−0.6	+
17	1946 Dec. 21	Nankaido	8.1	7.2～8.0	22	0.036	46	5.7～6.0	−0.6～+1.0	+
18	1952 Mar. 4	Tokachi-oki	8.1	3	22	0.02	3.7	12.8	+0.2	+
19	1952 Nov. 4	Kamchatka	8.2	14～15	17	0.058	60	6.9～7.1		+
20	1953 Nov. 26	Boso-oki	7.5	0.14～0.7	16	0.025	10	1.7～3.8		+
21	1960 May 22	Chile	8.5	30～75	—	—	138*	5.7～10	−2～+2	+
22	1960 Feb. 27	Fiuganada	7.2	**0.007**	428	0.01	1.6	0.9		+
23	1963 Oct. 13	Iturup	7.9	**1.2**	42	0.034	42	2.3		+
24	1964 May 7	W. Aomori	6.9	**0.003**	600	0.02	3	0.5		+
25	1964 June 16	Niigata	7.4	**0.2**	50	0.009	2.7	3.9	−4～+5**	+

* Aftershock area
** Sea bottom deformation.

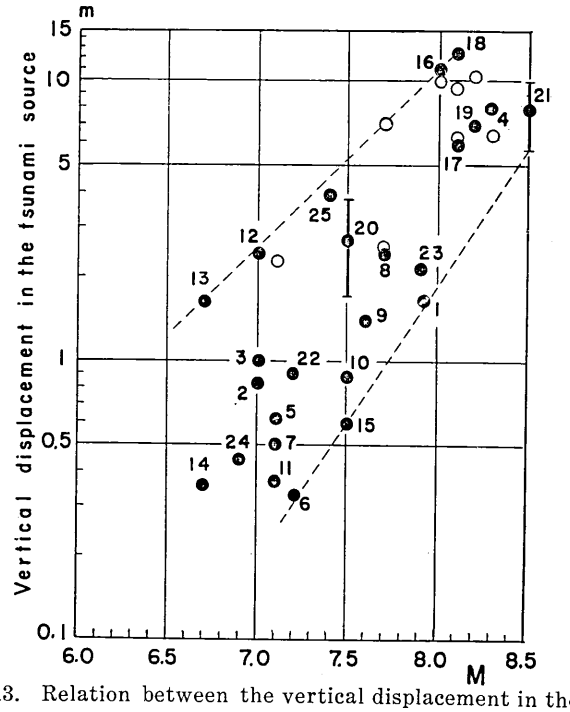

Fig. 13. Relation between the vertical displacement in the source and the earthquake magnitude.

The calculated displacements are compared with the observed maximum crustal deformation in Table 1. In cases of Kanto, Oga and Niigata Earthquakes for which the tsunami sources are close to the coast calculated values are approximately the same as the actual vertical displacement on land or the sea bottom.

The initial motion of the tsunami waves is mostly an up-wave except for a few cases in which leading waves begin with a down motion (Table 1), suggesting that the upward displacement of the bottom is more frequent than the downward displacement.

6. Conclusion

The source areas of tsunamis are shown on a bathymetric chart. The source areas are mostly located on the continental slope with the major axis of a source area along the contour line, but some are on the shelf or in the deep trench.

Tsunami energy seems to be affected by the slope of the sea bottom as well as by the water depth in the source, i.e. the energy of tsunami

generated in shallow water, for which the crustal deformation is partly on land, is relatively small for a given magnitude of the earthquake as experienced at the time of the Kanto and Oga Earthquakes.

From the distribution of the inundation heights near a tsunami source, a profile of the sea bottom deformation can be, roughly speaking, estimated. The average vertical displacement in a tsunami source estimated by using the tsunami energy and the source area is of the order of several meters for large tsunamis.

The author thanks Prof. K. Kajiura for his guidance.

References

1) N. MIYABE, "An Investigation of the Sanriku Tsunami Based on Mareogram Data," *Bull. Earthq. Res. Inst., Suppl.*, **1** (1934), 112.

2) F. KISHINOUYE and K. IIDA, "The tsunami that accompanied the Oga Earthquake of May 1, 1939," *Bull. Earthq. Res. Inst.*, **17** (1939), 733.

3) N. MIYABE, "Tsunami associated with the Earthquake of August 2, 1940," *Bull. Earthq. Res. Inst.*, **19** (1941), 104, (in Japanese).

4) S. OMOTE, "The Tsunami, the Earthquake Sea Waves, that accompanied the Great Earthquake of Dec. 7, 1944," *Bull. Earthq. Res. Inst.*, **24** (1946), 31, (in Japanese).

5) S. OMOTE, "On the Central Area of Seismic Sea Waves," *Bull. Earthq. Res. Inst.*, **25** (1947), 15.

6) Z. SUZUKI and K. NAKAMURA, "On the Heights of the Tsunami on March 4, 1952, in the District near Erimo-misaki," *Sci. Rep. Tohoku Univ. Geophysics*, [v], **4** (1953), 139.

7) K. IIDA, "Earthquakes accompanied by Tsunamis occurring under the Sea off the Islands of Japan." *J. Earth Sci., Nagoya Univ.*, **4** (1956), 1.

8) R. TAKAHASI and T. HATORI, "On the Tsunami which accompanied the Hiuganada Earthquake of Feb. 27, 1961." *Bull. Earthq. Res. Inst.*, **39** (1961), 561, (in Japanese).

9) С. А. Федотов "Определения областей возникновения волн цунами при Камчатском землетрясении 4 ноября 1952 г. и Итурупском землетрясении 6 ноября 1958 г." АН СССР, сер. геофиз., **10** (1962), 1333.

10) I. AIDA, K. KAJIURA, T. HATORI and T. MOMOI, "A Tsunami accompanying the Niigata Earthquake of June 16, 1964," *Bull. Earthq. Res. Inst.*, **42** (1964), 741, (in Japanese).

11) S. L. SOLOV' EV, "The Urup Earthquake and Associated Tsunami of 1963," *Bull. Earthq. Res. Inst.*, **43** (1965), 103.

12) T. HATORI, "On the Tsunami which accompanied the Earthquake off the Northwest of Oga on May 7, 1964," *Bull. Earthq. Res. Inst.*, **43** (1965), 149.

13) K. IIDA, "Magnitude, Energy, and Generation Mechanisms of Tsunamis and a Catalogue of Earthquakes associated with Tsunamis," *Proceeding of the Tsunami meeting associated with the Tenth Pacific Science Congress, IUGG Monograph*, No. **24** (1963), 7.

14) K. NAKAMURA and M. SUZUKI, "On the Character of Tsunami Waves Generated in a Sloped Region of the Ocean." *Sci. Rep. Tohoku Univ., Geophysics* [v], **16** (1965), 108.

15) K. IIDA, "A Relation of Earthquake Energy to Tsunami Energy and the Estimation of the Vertical Displacement in a Tsunami Source." *J. Earth Sci., Nagoya Univ.*, **11** (1963), 49.

16) H. WATANABE, "Studies on the Tsunamis on the Sanriku Coast of Northeastern Honshu in Japan," *Geophys. Mag.*, **32** (1964), 52.

17) T. MATUZAWA, *Study of Earthquakes*, (Tokyo, 1964), pp. 15-29.

18) T. TERADA and S. YAMAGUTI, "On the Propagation of Tsunami originated in Sagami Bay," *Rep. Imp. Earthq. Inv. Comm.*, **100**, **B** (1925), 113, (in Japanese).

19) CENTRAL METEOROLOGICAL OBSERVATORY, "The Boso-oki Earthquake of November 26, 1953," *Quart. J. Seism.*, **19** (1954), 42, (in Japanese).

20) R. TAKAHASI, "An Estimate of Future Tsunami Damage along the Pacific Coast of Japan," *Bull. Earthq. Res. Inst.*, **29** (1951), 71.

21) T. HATORI, "On the Tsunami which accompanied the Niigata Earthquake of June 16, 1964.—Source Deformation, Propagation and Tsunami Run-up," *Bull. Earthq. Res. Inst.*, **43** (1965), 129.

---

70. 津波の波源域における海底地形と変動

地震研究所　羽鳥徳太郎

1933年の三陸津波について，宮部 (1934) は各地の検潮記録をもとに，津波の逆伝播図をえがき，波源域を推定した．この結果，波源はかなり広い領域をもつたことが明らかにされた．以来，多くの人達によつて，同様な方法で，二十数個の津波の波源域が推定されてきている．今回，1923年の関東地震および1953年の房総沖地震に伴なつた津波の波源域を逆伝播図によつて推定したところ，その長径はそれぞれ約 170 km および 160 km である．また関東地震の場合，その波源域は三浦半島および房総半島の隆起地帯を大きく包含し，房総沖地震の波源域は，その余震域とかなりよく一致している．

これらの推定された波源域を海図上に図示すると，多くは陸棚斜面に分布し，大地震の多発地帯でもあるが，大きな津波は波源域の平均水深の深いところに発生している傾向がある．次に波源域における平均的の海底傾斜と E_s/E_t (E_s：地震波のエネルギー，E_t：津波エネルギー) との関係を図示すると，津波エネルギーは発生メカニズムのほかに，海底の傾斜による効果をある程度受けるようにみえる．

地形変動が実測された 2, 3 の津波について，波源縁上の波高を Green の方法で沿岸の波高から計算した．海岸に沿つた地形変動と，それに対応する波高計算値とを対比すると，両者の分布形状は大局的に類似を示す．すなわち波源近傍の，沿岸効果をとり除いた波高分布から，海底変動の一断面が推測できそうである．

次に海底変動が突然起つたとすると，波源のポテンシャル・エネルギーは，海底の平均的な変動量を Z, 波源の面積を S とすれば

$$E_t=\frac{1}{2}\rho g Z^2 S$$

で，おおよそ表わされる．波源の面積と検潮記録から求められている津波エネルギーのデータを用い，上式から各津波の平均的な海底変動量を計算して，変動の実測値と比較を行なつた．さらに地震のマグニチュードとの関係をみると，大きな津波の海底変動はメーターのオーダーと思われる．